THE UNIVERSITY OF WESTERN AUSTRALIA

Research Report of Intelligent Systems for Medicine Laboratory

Report # ISML/03/2017, March 2017

Maximum Principal AAA Wall Stress is Proportional to Wall Thickness

K. Miller, G. Joldes, J. Qian, A.P. Patel, M.S. Jung and A. Wittek

Intelligent Systems for Medicine Laboratory
School of Mechanical Engineering
The University of Western Australia
35 Stirling Highway
Crawley WA 6009, AUSTRALIA
Phone: + (61) 8 6488 1901
Fax: + (61) 8 6488 1024
Email: karol.miller@uwa.edu.au
http://isml.ecm.uwa.edu.au/

Keywords: Abdominal Aortic Aneurysm; Patient-Specific Modelling; Finite Element Method; Stress; Wall Thickness

Abstract:

Abdominal aortic aneurysm (AAA) is a permanent and irreversible dilation of the lower region of the aorta. It is a symptomless condition that if left untreated can expand to the point of rupture. Mechanically-speaking, rupture of an artery occurs when the local wall stress exceeds the local wall strength. It is therefore desirable to be able to estimate the AAA wall stress for a given patient non-invasively, quickly and reliably.

Recently our Intelligent Systems for Medicine Laboratory (ISML) and a group from Oregon presented a very efficient method to compute AAA wall stress using geometry from CT and median arterial pressure for a load. The ISML's method is embedded in the software platform *BioPARR - Biomechanics based Prediction of Aneurysm Rupture Risk*, freely available from http://bioparr.mech.uwa.edu.au/. Experience with over fifty patient-specific stress analyses as well as common sense suggest that the AAA wall stress critically depends on the local AAA wall thickness. This thickness is currently very difficult to measure in the clinical environment. Therefore, we conducted a simulation study to elucidate the relationship between the wall thickness and the maximum principal stress. The results of the analysis of three cases presented here unequivocally demonstrate that this relationship is approximately linear, bringing us closer to being able to compute predictive stress envelopes for every patient.

1 Introduction

Abdominal aortic aneurysm (AAA) is a permanent and irreversible dilation of the lower region of the aorta. It is typically a symptomless condition that if left untreated, can result is a rupture of an aorta. AAA diagnosis has tripled over the last thirty years and is likely to continue increasing (Bosch et al. 2002). AAA is found in approximately 7% of elderly men (>65 yrs) in Australia (Norman et al. 2004) with similar prevalence in the Western world (Singh et al. 2001). This equates to about 114,000 Australian men currently living with AAA. GBE-Bund statistics shows that in 2014 the number of hospitalized AAA patients in Germany was about 85400. The disease also affects women, but to a lesser rate.

As AAA is typically asymptomatic, most people are unaware of their condition. However, AAA rupture is a catastrophic clinical event with mortality rates of approximately 80-90% (Bengtsson et al. 1993, Kantonen et al. 1999, Evans et al. 2000). Currently, the most evidence-based indicator of rupture threat is the maximum anterior-posterior diameter. Diameters >5.5cm are deemed high risk. Yet, 20% of smaller AAAs rupture and larger cases often remain quiescent (Darling et al. 1977, Greenhalgh). Surgical repairs of AAA are expensive. They cost the Australian health system approximately $230m per year and as many as 75% of these operations may be unnecessary. The ability to predict, non-invasively, which cases are at risk of rupture will have a major clinical impact by saving lives and reducing medical costs worldwide.

There are many limitations to the current clinical definition of ‘high-risk’ and many researchers believe that patient-specific modelling (PSM) could have major clinical potential (McGloughlin et al. 2010, Vande Geest et al. 2006, Gasser et al. 2010, Gasser et al. 2014, Joldes et al. 2016, Zelaya et al. 2014). Mechanically-speaking, rupture of an artery occurs when the local wall stress exceeds the local wall strength. With the advances in medical imaging technology and medical image analysis software, it has become possible to create patient-specific reconstructions of the AAA, which were then used for computer simulations aiming at computing the wall stress that have steadily increased in complexity (Gasser, Auer 2010, Raghavan et al. 2000, Doyle et al. 2007, Li et al. 2010). Major research efforts have been preoccupied with material models and simulations so comprehensive that they require computer power and specialist knowledge to implement inaccessible in a typical clinic.

Recently, an entirely new, very simple approach to compute AAA wall stress was proposed and validated in (Joldes, Miller 2016) (see also (Zelaya, Goenezen 2014, Fung 1991)). The inputs to the model are the (loaded) geometry of an aneurysm (obtained from a CT reconstruction), wall thickness and blood pressure. The method is embedded in the software platform *BioPARR - Biomechanics based Prediction of Aneurysm Rupture Risk*, freely available from http://bioparr.mech.uwa.edu.au/. What is truly exciting about this simple approach is that one does not need any information on arterial tissue material parameters; this supports the development and use of PSM, where uncertainty in material data, until recently (Miller et al. 2013), has been recognized as a key limitation. Moreover the computation itself is so simple that many repeated simulations for a single patients are feasible, enabling a stochastic extension of the models (Calvetti et al. 2014).

The accuracy, predicative power and ultimately clinical utility of this simple and efficient method to compute AAA wall stress critically depends on the ability to estimate AAA wall thickness. At present all patient-specific computational biomechanics studies in the field of vascular biomechanics assume homogeneous and constant wall thickness. However, recently (Zhu et al. 2016) demonstrated novel MR imaging technique that may lead to a more accurate thickness measurement. In (Joldes, Miller 2016) we undertook one of the first attempts of measuring AAA wall thickness via a CT-MRI fusion. In this paper, starting form this imperfect measurement of wall thickness, we evaluate the relationship between the AAA wall thickness and the maximum principal stress.

2 Methods

Complete stress analyses of AAA were conducted using our freely available software BioPARR (http://bioparr.mech.uwa.edu.au/). Excluding the 3D reconstruction time, the entire analysis of a single load case scenario took approx. 6 minutes on an Intel(R) Core(TM) i7-5930K CPU @ 3.50GHz with 64GB of RAM running Windows 8 OS. The analysis steps are briefly described below.

2.1 Problem Geometry

We used three real-world, patient-specific 3D geometries, sourced from the initial phase of the MA3RS study (McBride et al. 2015), with all the irregularities that can be expected in clinical

simulations, Figure 1.

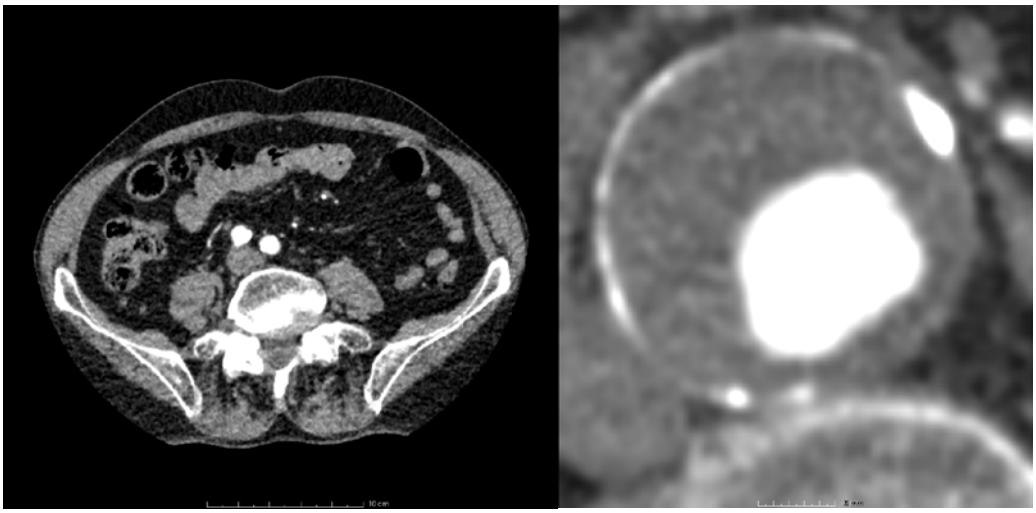

Figure 1. An example AAA case considered in this study. a) CT image; b) Region of interest, showing the lumen and portions of the AAA wall in white and intraluminal thrombus (ILT) in gray.

Our software system BioPARR allows the analyst to extract and combine data from images of different modality (such as CT and MRI), by implementing an segmentation based inter-modality image registration algorithm in 3D Slicer (Fedorov et al. 2012), as shown in Figure 2. The analyst has control over many parameters influencing the analysis results: the thickness of the AAA wall, inclusion of thrombus, geometry meshing, finite element type selection, and finite element simulation scenarios. The software can be used in the case when both CT and MRI data are available for a patient or, the more typical situation, when only CT is acquired: CT images are acquired as part of routine care and are available for most clinically relevant AAAs.

The program automatically generates 3D color-contoured visualizations of the key patient-specific components of the analysis, namely, ILT thickness and the normalized ratio of the maximum AAA diameter and the diameter in the proximal neck of the aneurysm (NORD).

2.2 Image Segmentation

The high variability in AAA geometry, as well as low discrimination between the AAA and the surrounding tissue in parts of the image, make automatic AAA segmentation practically

impossible. Therefore, our software uses segmentation tools available in the free, open source image analysis software 3D Slicer (Fedorov et al. 2012). We have found that using the 3D Slicer extension FastGrowCut for segmentation (Zhu et al. 2014) can help reduce the segmentation time. Manual intervention is still required in defining the region of interest in the image, cropping, defining the seeds for the FastGrowCut algorithm and performing corrections and smoothing of the resulting label maps. Using this method, we can extract the AAA geometry from CT or MRI.

2.4 Wall thickness measurement and specification

Although wall thickness has a great influence on the stress distribution within the AAA wall (Joldes et al. 2016), accurate extraction from medical images remains problematic due to the low image resolution and the fact that, because of having similar intensity in the image, it is very difficult to distinguish the AAA wall from parts of the surrounding tissue. This uncertainty is why many authors have used constant wall thickness in their analyses. BioPARR offers the possibility of specifying wall thickness at multiple points on the AAA surface. These discrete thickness measurements are then converted to a smooth model of an aneurysm wall through interpolation.

The uncertainty in the patient-specific AAA wall thickness will propagate through the computational model and result in uncertainty in the computed stress. Therefore, for each case considered we conducted repeated manual measurements of wall thickness in three cross-sections, where the image contract was best and reasonable accuracy could be attained, Figures 2 and 3.

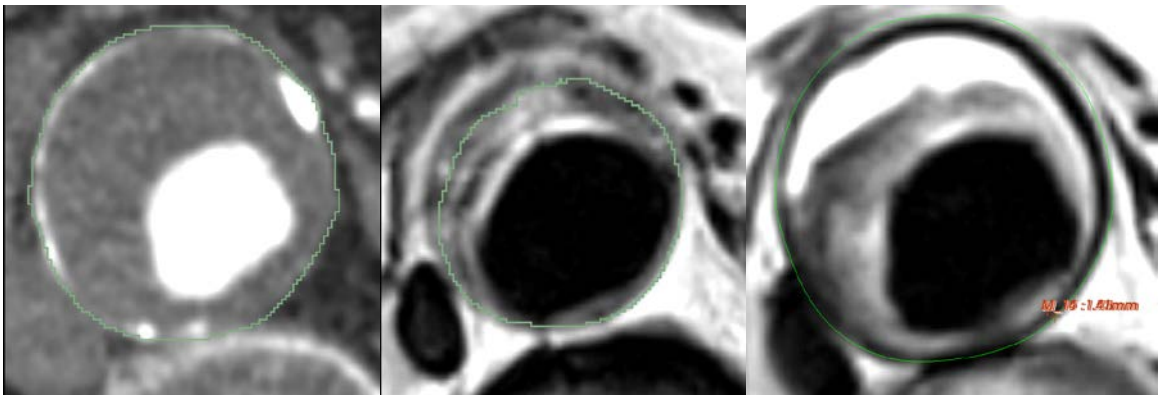

Figure 2: MRI to CT registration. Axial view of AAA label map (green contour) segmented from CT (left); Axial view of AAA label map segmented from MRI (centre); CT label map over MRI image demonstrated the quality of MRI to CT registration (right).

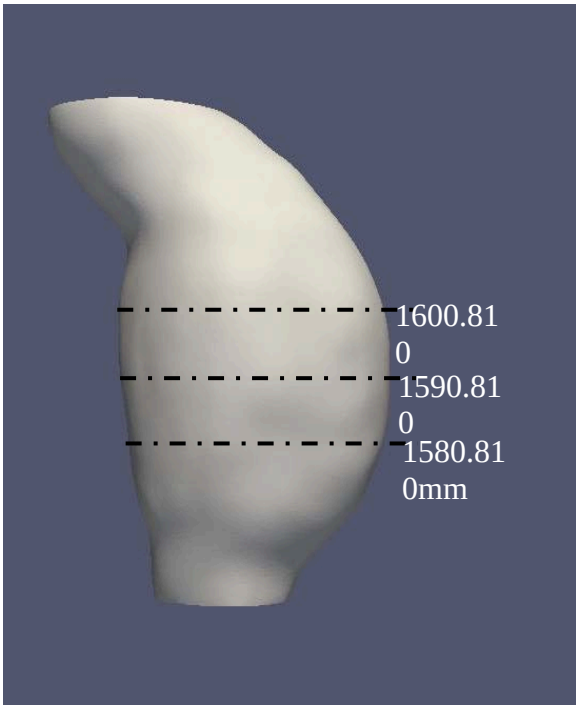

Figure 3. Cross-sections at which repeated measurements of AAA wall thickness were conducted. Five measurements were taken at two points in each cross-section using the MRI image registered to CT.

Estimated variable wall thickness for Case 1 is given in Fig. 4. It is clear that the wall thickness may vary locally from as little as 1.4 mm to about 2.1 mm.

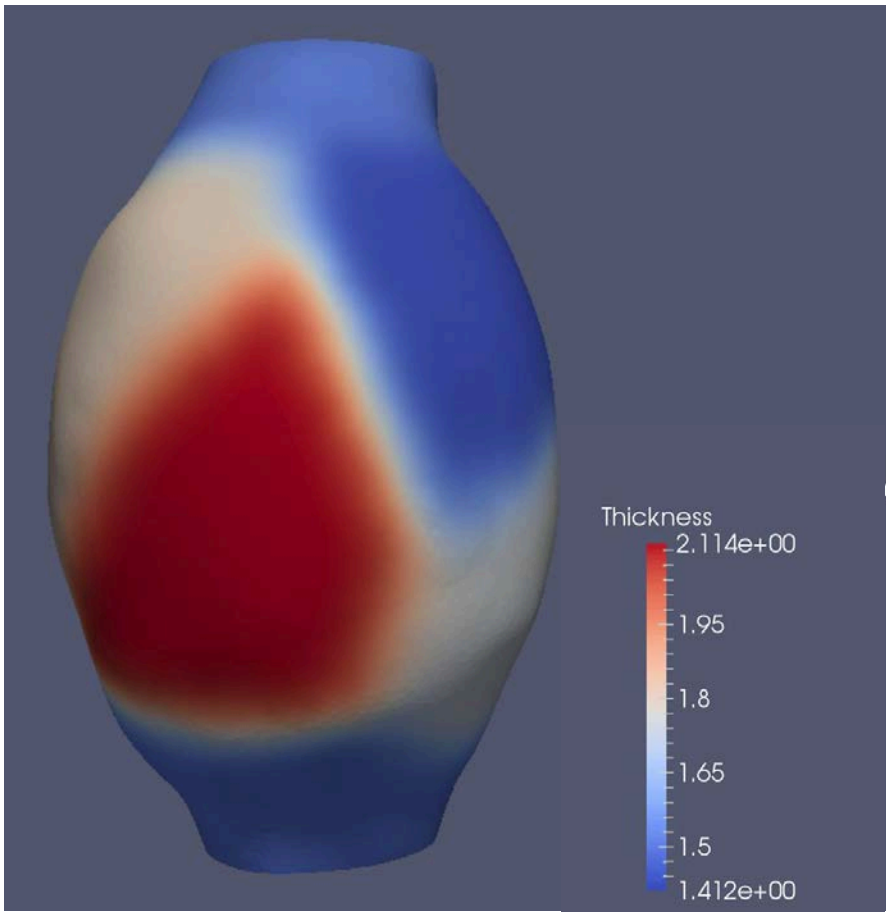

Figure 4: AAA Geometry (Case 1) generated using varying thickness. Measured thickness varies between 1.4 mm and 2.11 mm for this case.

2.5 Geometry creation

The label maps segmented from images and the wall thickness information are used to create the AAA geometry. The external AAA wall surface, the internal AAA wall surface and the internal intraluminal thrombus (ILT) surface are automatically created.

2.6 Finite Element Meshing, Model Creation and Analysis

Meshing of the AAA wall and ILT, based on external and internal AAA wall surfaces and the internal ILT surface, is performed using open source meshing software Gmsh (Geuzaine et al. 2016, Geuzaine et al. 2009) called from within BioPARR. A tetrahedral volumetric mesh is

created using the element size specified by the user. This process ensures a conforming mesh between the ILT and AAA wall. Meshing approach implemented in BioPARR maintains the geometric accuracy of the meshed surfaces by using very small elements on these surfaces. At the same time, by increasing the element size inside the ILT volume and in the thicker areas of the AAA wall, it reduces the mesh size and, therefore, the computational cost of the finite element analysis.

The element types can be configured as linear or quadratic, displacement only or hybrid displacement-pressure formulation. Finally, Abaqus (ABAQUS 2009) input (.inp) files are generated and sent for finite element analysis. Figure 6 shows a typical AAA mesh.

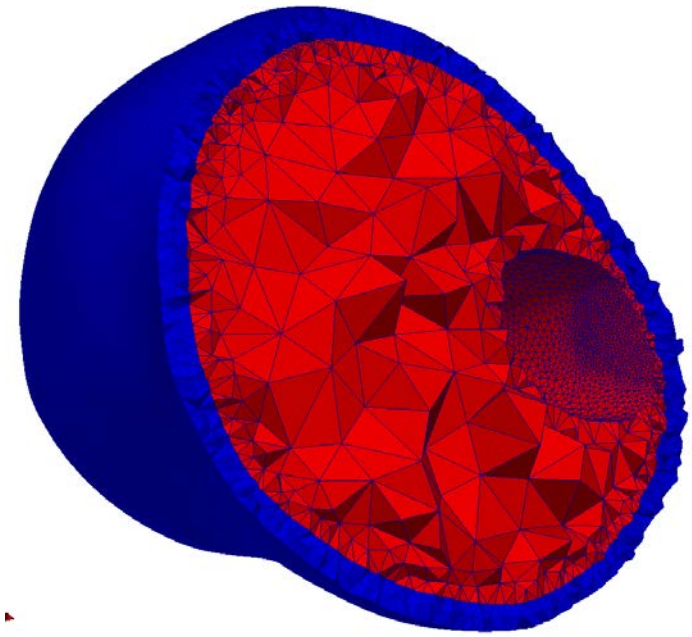

Figure 5. **Example of meshing.** The AAA wall is meshed using 2 layers of elements (configurable). The ILT is meshed using a minimum of 2 layers of elements (configurable); the element size is increased in the middle of the ILT layer to reduce the number of elements in the mesh.

The finite element simulations are carried out using the procedure described in (Joldes, Miller 2016), which allows the computation of stress in the AAA wall without exact knowledge about the material properties. This is of great practical significance, as patient-specific material properties for the AAA wall and ILT are currently impossible to obtain *in vivo*. For a detailed discussion of

the problem of obtaining solutions without knowing mechanical properties of tissues please see also (Miller and Lu 2013, Wittek et al. 2009).

The results of finite element simulations (maximum principal stresses in the AAA wall) are extracted by BioPARR for visualization and analysis.

3 Results

For each case considered we conducted five thickness measurements at six points on the AAA wall. The measurements where then ranked from the smallest to the largest. We then created five geometries (as explained in the Methods section) using measured thicknesses with the same rank. This allowed us to create five finite element models, ranked by average wall thickness, for each of the three cases considered in this study.

We chose to use maximum principal stress as a scalar indicator of the internal forces being withstood by the wall tissue. Typical results are given in Figure 6.

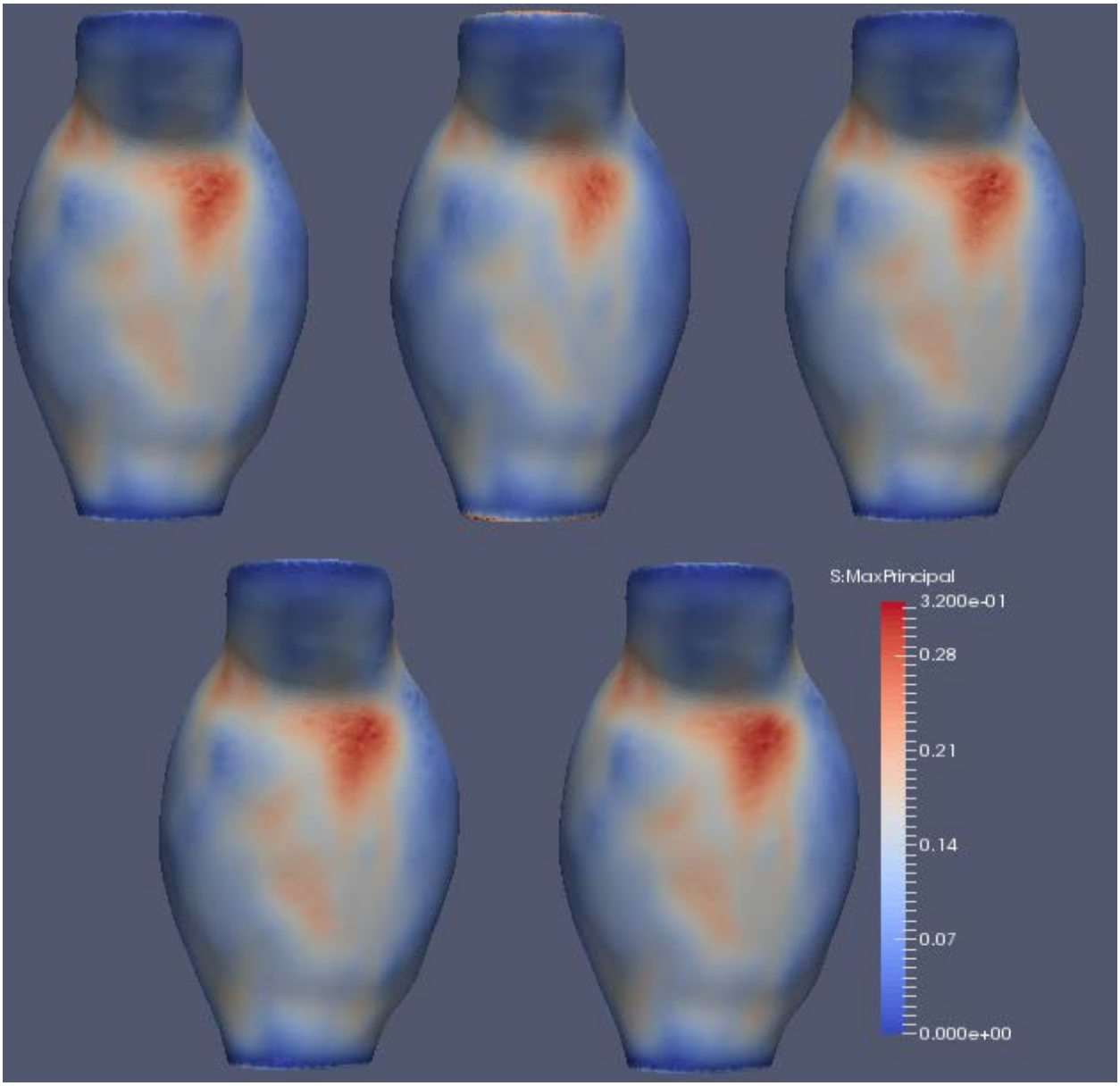

Figure 6: Maximum principal stress for Case 1. From the thickest (top left), to the thinnest wall (bottom right)

In Figure 7 we present the relationship between the maximum principal wall stress and the average wall thickness. It is clear that this relationship, for every case considered, is approximately linear.

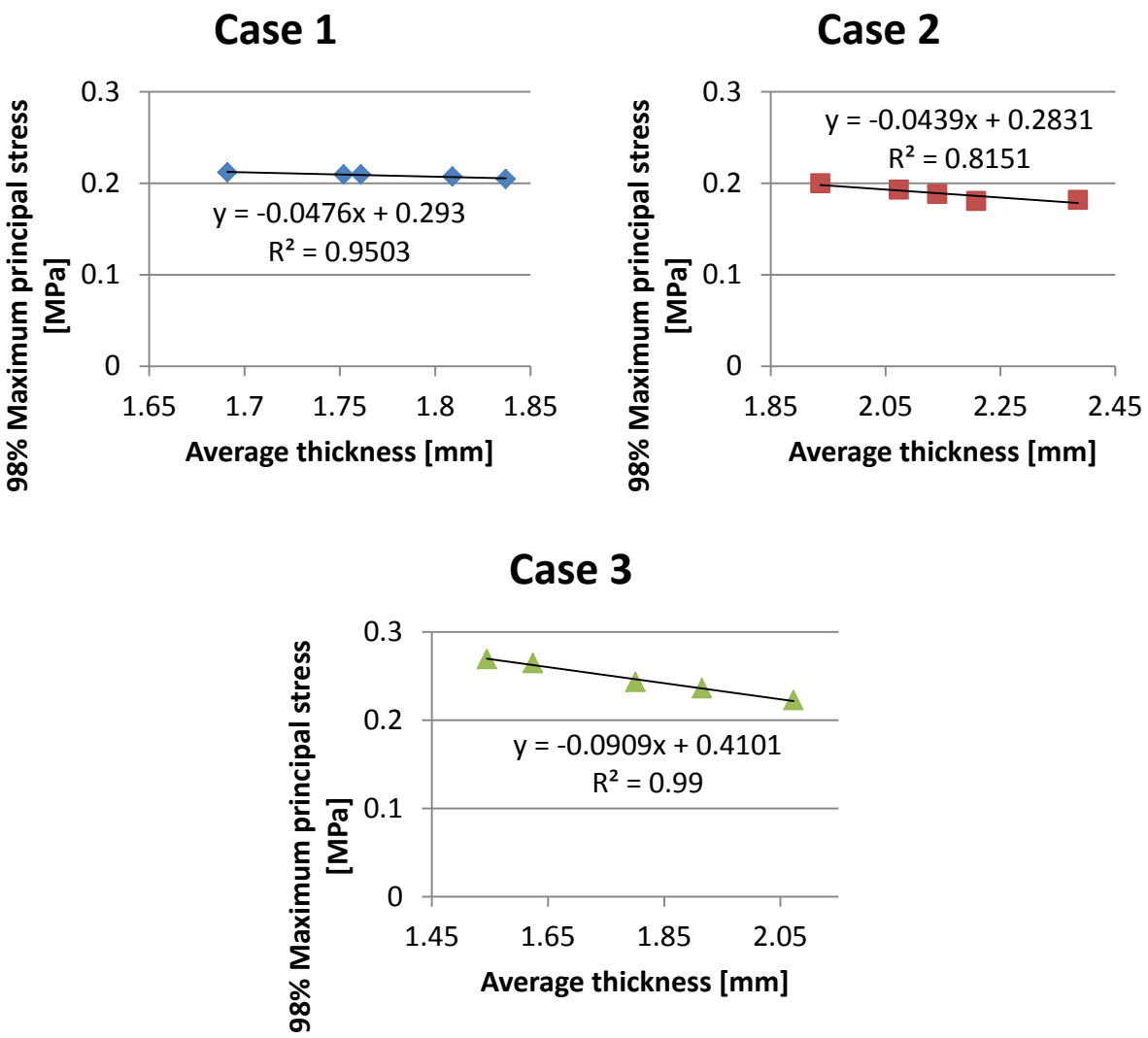

Figure 7: Relationship between the average AAA wall thickness and maximum principal stress (98 percentile) for the analyzed cases.

4 Discussion and Conclusions

We used our recently developed and made publically available software BioParr (http://bioparr.mech.uwa.edu.au/) to analyse the relationship between the difficult to measure AAA wall thickness and the wall stress. Our results indicate that this relationship is approximately linear. The simplicity of this relationship allows certain level of optimism with regard to the possibility of confidently constructing predictive stress envelopes for individual AAA patients.

The result presented in this paper is not entirely surprising. Standard engineering equations for

stress in cylindrical pressure vessels exhibit linearity between vessel wall thickness and maximum stress. Also the following simple dimensional reasoning, which we owe to Dr. Johann Drexl from Fraunhofer MEVIS, suggests that our results, even though computed for complicated geometries, are not entirely unexpected. Blood pressure acts on the internal surface of an aneurysm whose area is proportional to the square of the AAA radius. Internal forces (stresses), balancing the pressure load, act on the cross-section of the AAA wall which is proportional to the radius multiplied by the wall thickness. Therefore the linear variation of stress with the wall thickness is not entirely unexpected.

The presented result is in agreement with our suggestion from over ten years ago that in biomechanics often seemingly very complicated relationships conceal an approximately linear dependence (Taylor et al. 2005).

Acknowledgements

The financial support of the National Health and Medical Research Council (Grant No. APP1063986) is gratefully acknowledged. We wish to acknowledge the Raine Medical Research Foundation for funding G. R. Joldes through a Raine Priming Grant. The AAA data has been obtained from the MA3RS study (McBride, Berry 2015).

References

[1] Bosch J. L., Kaufman J. A., Beinfeld M. T., Adriaensen M. E. A. P. M., Brewster D. C., Gazelle G. S. (2002) *Abdominal Aortic Aneurysms: Cost-effectiveness of Elective Endovascular and Open Surgical Repair*. Radiology; **225**(2): 337-344.

[2] Norman P. E., Jamrozik K., Lawrence-Brown M. M., Le M. T. Q., Spencer C. A., Tuohy R. J., Parsons R. W., Dickinson J. A. (2004) *Population based randomised controlled trial on impact of screening on mortality from abdominal aortic aneurysm.* BMJ; **329**(7477): 1259.

[3] Singh K., Bønaa K. H., Jacobsen B. K., Bjørk L., Solberg S. (2001) *Prevalence of and Risk Factors for Abdominal Aortic Aneurysms in a Population-based Study: The Tromsø Study*.

American Journal of Epidemiology; **154**(3): 236-244.

[4] Bengtsson H., Bergqvist D. (1993) *Ruptured abdominal aortic aneurysm: A population-based study*. Journal of Vascular Surgery; **18**(1): 74-80.

[5] Kantonen I., Lepäntalo M., Brommels M., Luther M., Salenius J. P., Ylönen, the Finnvasc Study Group K. (1999) *Mortality in Ruptured Abdominal Aortic Aneurysms.* European Journal of Vascular and Endovascular Surgery; **17**(3): 208-212.

[6] Evans S. M., Adam D. J., Bradbury A. W. (2000) *The influence of gender on outcome after ruptured abdominal aortic aneurysm.* Journal of Vascular Surgery; **32**(2): 258-262.

[7] Darling R. C., Messina C. R., Brewster D. C., Ottinger L. W. (1977) *Autopsy study of unoperated abdominal aortic aneurysms. The case for early resection.* Circulation; **56**: 161-164.

[8] Greenhalgh R. M. (2004) *Comparison of endovascular aneurysm repair with open repair in patients with abdominal aortic aneurysm (EVAR trial 1), 30-day operative mortality results: randomised controlled trial.* The Lancet; **364**(9437): 843-848.

[9] McGloughlin T. M., Doyle B. J. (2010) *New Approaches to Abdominal Aortic Aneurysm Rupture Risk Assessment: Engineering Insights With Clinical Gain.* Arteriosclerosis, Thrombosis, and Vascular Biology; **30**(9): 1687-1694.

[10] Vande Geest J. P., Di Martino E. S., Bohra A., Makaroun M. S., Vorp D. A. (2006) *A biomechanics-based rupture potential index for abdominal aortic aneurysm risk assessment: demonstrative application.* Annals of the New York Academy of Sciences; **1085**: 11-21.

[11] Gasser T. C., Auer M., Labruto F., Swedenborg J., Roy J. (2010) *Biomechanical rupture risk assessment of abdominal aortic aneurysms: model complexity versus predictability of finite element simulations.* European Journal of Vascular and Endovascular Surgery; **40**(2): 176-85.

[12] Gasser T. C., Nchimi A., Swedenborg J., Roy J., Sakalihasan N., Bockler D., Hyhlik-Durr A. (2014) *A novel strategy to translate the biomechanical rupture risk of abdominal aortic aneurysms to their equivalent diameter risk: method and retrospective validation.* Eur J Vasc Endovasc Surg; **47**(3): 288-95.

[13] Joldes G. R., Miller K., Wittek A., Doyle B. (2016) *A simple, effective and clinically applicable method to compute abdominal aortic aneurysm wall stress.* Journal of the mechanical behavior of biomedical materials; **58**: 139-148.

[14] Zelaya J. E., Goenezen S., Dargon P. T., Azarbal A.-F., Rugonyi S. (2014) *Improving the Efficiency of Abdominal Aortic Aneurysm Wall Stress Computations.* PLoS ONE; **9**(7): e101353.

[15] Raghavan M., Vorp D., Federle M., Makaroun M., Webster M. (2000) *Wall stress distribution on three-dimensionally reconstructed models of human abdominal aortic aneurysm.* J Vasc Surg; **31**: 760 - 769.

[16] Doyle B., Callanan A., McGloughlin T. (2007) *A comparison of modelling techniques for computing wall stress in abdominal aortic aneurysms.* Biomed Eng Online; **6**(1): 38.

[17] Li Z. Y., Sadat U., J U. K.-I., Tang T. Y., Bowden D. J., Hayes P. D., Gillard J. H. (2010) *Association between aneurysm shoulder stress and abdominal aortic aneurysm expansion: a longitudinal follow-up study.* Circulation; **122**(18): 1815-22.

[18] Fung Y. C. (1991) *What Are the Residual Stresses Doing in Our Blood Vesssels?* Annals of Biomedical Engineering; **19**: 237-249.

[19] Miller K., Lu J. (2013) *On the prospect of patient-specific biomechanics without patient-specific properties of tissues.* Journal of the Mechanical Behavior of Biomedical Materials; **27**: 154–166.

[20] Calvetti D., Kaipio J. P., Somersalo E. (2014) *Inverse problems in the Bayesian framework.* Inverse Problems; **30**(11): 110301.

[21] Zhu C., Haraldsson H., Faraji F., Owens C., Gasper W., Ahn S., Liu J., Laub G., Hope M. D., Saloner D. (2016) *Isotropic 3D black blood MRI of abdominal aortic aneurysm wall and intraluminal thrombus.* Magnetic Resonance Imaging; **34**(1): 18-25.

[22] McBride O. M. B., Berry C., Burns P., Chalmers R. T. A., Doyle B., Forsythe R., Garden O. J., Goodman K., Graham C., Hoskins P., Holdsworth R., MacGillivray T. J., McKillop G., Murray G., Oatey K., Robson J. M. J., Roditi G., Semple S., Stuart W., van Beek E. J. R., Vesey A., Newby D. E. (2015) *MRI using ultrasmall superparamagnetic particles of iron oxide in patients under surveillance for abdominal aortic aneurysms to predict*

rupture or surgical repair: MRI for abdominal aortic aneurysms to predict rupture or surgery—the MA3RS study. Open Heart; **2**(1).

[23] Fedorov A., Beichel R., Kalpathy-Cramer J., Finet J., Fillion-Robin J.-C., Pujol S., Bauer C., Jennings D., Fennessy F., Sonka M., Buatti J., Aylward S., Miller J. V., Pieper S., Kikinis R. (2012) *3D Slicer as an image computing platform for the Quantitative Imaging Network.* Magnetic Resonance Imaging; **30**(9): 1323–1341.

[24] Fedorov A., Beichel R., Kalpathy-Cramer J., Finet J., Fillion-Robin J.-C., Pujol S., Bauer C., Jennings D., Fennessy F., Sonka M. (2012) *3D Slicer as an image computing platform for the Quantitative Imaging Network.* Magnetic Resonance Imaging; **30**(9): 1323-1341.

[25] Zhu L., Kolesov I., Gao Y., Kikinis R., Tannenbaum A. (2014) *An Effective Interactive Medical Image Segmentation Method Using Fast GrowCut*, in *International Conference on Medical Image Computing and Computer Assisted Intervention (MICCAI), Interactive Medical Image Computing Workshop*: Boston, USA.

[26] Joldes G. R., Miller K., Wittek A., Doyle B. (2016) *A simple, effective and clinically applicable method to compute abdominal aortic aneurysm wall stress.* Journal of the Mechanical Behavior of Biomedical Materials; **58**: 139–148.

[27] http://gmsh.info/, Gmsh - A three-dimensional finite element mesh generator with built-in pre- and post-processing facilities

[28] Geuzaine C., Remacle J.-F. (2009) *Gmsh: a three-dimensional finite element mesh generator with built-in pre- and post-processing facilities.* International Journal for Numerical Methods in Engineering; **79**(11): 1309-1331.

[29] ABAQUS (2009) *ABAQUS Theory Manual Version 6.9*, Providence, RI: Dassault Systèmes Simulia Corp.

[30] Wittek A., Hawkins T., Miller K. (2009) *On the unimportance of constitutive models in computing brain deformation for image-guided surgery*. Biomechanics and modeling in mechanobiology; **8**(1): 77-84.

[31] Taylor Z., Miller K. (2005) *Using numerical approximation as an intermediate step in analytical derivations: some observations from biomechanics.* Journal of biomechanics; **38**(12): 2497-2502.